Contents lists available at SciVerse ScienceDirect

Journal of Non-Crystalline Solids

Letter to the Editor

Enthalpy relaxation near the glass transition for comb-like polymer: Power law relaxation revealed by DSC experiment

Y. Tanaka [*], H. Asano, Y. Okuya

Department of Material Science and Engineering, Faculty of Engineering, University of Fukui, Fukui 910-8507, Japan

ARTICLE INFO

ABSTRACT

A series of enthalpy relaxation experiments at different ageing temperatures was conducted on a sample of poly(cyanobiphenyl hexylacrylate) with variation in the molecular weight using a DSC technique. The value of the relaxation function (ϕ) was obtained as a function of the ageing time (t_A) from the experimental results using the excess enthalpy in the limit of infinity of t_A and that of the given t_A. The double logarithmic plot of $-\ln\phi$ and t_A was constructed to determine the functional form of the relaxation function. Two possible forms are found, the stretched exponential and the power law forms, which suggests that the functional form varies continuously between these two according to the ageing experiment. The activation energy spectrum was derived for the two functional forms, which show the distribution of the activation energy of the molecular process controlling the decrease in enthalpy. It was revealed that, for the spectrum based on the power law relaxation, the overwhelming fraction of the relaxation processes is at the lower energy side and the population of the process decreases rapidly toward the higher energy side.

© 2012 Elsevier B.V. All rights reserved.

1. Introduction

The relaxation phenomenon in physical properties is often observed in a wide variety of substances. The phenomenon presents the decay process to the equilibrium states and is described by the function of time, i.e., the relaxation function, ϕ. The mathematical formulae usually used for the relaxation are the exponential forms, the single exponential, or double exponential functions [1,2]. On the other hand, the stretched exponential function expressed as Eq. (1) is frequently used to describe the non-exponential decay [3,4].

$$\phi = \exp[-(t_A/\tau)]^{\beta}; \quad 0<\beta\leq 1 \tag{1}$$

t_A and τ are the experimental ageing time and relaxation time, respectively. It is applicable to lots of experimental results and the stretch exponent, β, can be taken as a convenient measure of the many-body relaxation dynamics. In recent years, a modified response function expressed by a fractional function has been proposed by Avramov et al., to apply to the relaxation kinetics of glass-forming melts [5]. The nature of relaxation, the thermodynamic fragility, and rigidity of glass are related to the parameter included in the function

of Avramov. Therefore, the physical nature is incorporated into the proposed equation.

Apart from very few exceptions, the stretched exponential form is usually used for the relaxation in the glass transition of polymer. In contrast, in this work is presented the possibility that the power function is applicable to the enthalpy relaxation measured using the DSC technique.

$$\phi = A \times (t_A)^{-n}; 0<n\leq 1, \lambda_0<t_A\leq\infty. \tag{2}$$

The exponent, n, characterise the distribution of relaxation modes [6]. λ_0 is a time constant that depends on the material structure. Because many simulation studies show that the power law decay is observable for the relaxation in the glass transition, it is conceivable that the power function describes the decay curve in the enthalpy relaxation [7–9]. As a matter of fact, the experimental result has, as far as we know, not been reported before for the power law relaxation in the glass formation.

In previous studies, we also examined the decrease in enthalpy, $\Delta H(t_A, T_A)$, upon the ageing experiment on the basis of the stretched exponential function [10,11]. The double logarithmic plot of $-\ln\phi$ vs. t_A was constructed for the data of $\Delta H(t_A, T_A)$ since this plot is convenient to determine the parameters of β and τ. T_A is the ageing temperature, and t_A, the ageing time. In preparing the plot, we found that several data sets may be fitted with the power law behaviour. The stretched exponential form is given by a straight line; the power law form, by a gentle upward convex curve on the double logarithmic plot. Occasionally, there were nearly no differences between the

* Corresponding author. Tel.: +81 776 27 8974; fax: +81 776 27 8767.
E-mail address: tanaka@matse.u-fukui.ac.jp (Y. Tanaka).

straight line and the gentle curve. However, all the $\Delta H(t_A, T_A)$ data were analysed with the stretched exponential form in previous papers. The present short communication reports the power law behaviour indicated by the upward convex curve on the $-\ln\phi$ vs. t_A plot. Previously published data of $\Delta H(t_A, T_A)$ were used again in the present study to contrast these two functions. To evaluate the uncertainties of $\Delta H(t_A, T_A)$, the measurements were repeated with new specimens.

The sample used is a comb-like polymer, which has the cyanobiphenyl group as the mesogenic unit in the side chain (PCB6A). The reason for examining the liquid crystalline polymer is the significant variation of the free volume in the glass transition, which is expected to lead to an observable enthalpy decrease upon experimental time. Research reports on enthalpy relaxation exist for samples of liquid crystalline polymers of the side-chain type, presumably with similar reasons [12–14]. Moreover, the relaxation process is characterised in terms of the activation energy spectrum (AES) model [10,15]. AES demonstrates the density of the molecular processes which control the progress of the enthalpy change during the isothermal stage.

2. Experimental section

The PCB6A samples shown in Table 1 were prepared by radical polymerisation from the monomer 6-(4′-cyanobiphenyl-4-yloxy) hexyl-acrylate. The polymer obtained was fractionated by GPC. All the samples show the same nematic–isotropic transition point (T_{N-I}) of 129 °C. Detailed descriptions of the sample preparation, determination of the molecular weight, and specific heat increment between glassy and the liquid states (Δc_p) can be seen in a previous paper [10]. T_g is determined from the value of enthalpic T_g, namely, the cross point using the two extrapolation lines drawn over the plot of the enthalpy and temperature for the glassy and the liquid states of sample [16,17]. The method to verify the enthalpy loss was also conducted to ensure the location of T_g [10].

To acquire comparable data, a consistent temperature programme was applied to the PCB6A sample using a DSC instrument (SEIKO DSC200) The sample was (i) first maintained at 160 °C, well above T_{N-I} for 5 min to erase any previous thermal history; (ii) cooled to a specified ageing temperature, T_A, with a cooling rate of 12 °C/min; (iii) annealed for the ageing period t_A; and (iv) cooled to $T_1 = -20$ °C, well below T_g. Then, the DSC curve was recorded on heating at a rate of 5 °C/min to determine $\Delta H(t_A, T_A)$, namely, the enthalpy loss associated with the ageing process of (iii) [17,18]. Before each measurement, the reference scan was recorded following steps (i), (ii), and (iv), i.e., the scan without the ageing. The setting for T_A was in the range of 13 to 33 °C with an interval of 5 °C.

The DSC curve was transformed to the $c_p(T)$ curve, where the calibration was carried out with reference to c_p of indium of 200, 250, 298, 400, and 500 K. c_p data of the scan following the ageing process of (iii) are denoted by $c_{p,age}$; the data without the process of (iii) are

denoted by $c_{p,ref}$. The expression for $\Delta H(t_A, T_A)$ is then written as follows with T^*, a temperature high enough to accept that the sample is in equilibrium [19].

$$\Delta H(t_A, T_A) = \int_{T_1}^{T_*} \left(c_{p,age} - c_{p,ref} \right) dT. \tag{3}$$

For $\Delta H(\infty, T_A)$, the limiting value of $t_A \to \infty$, can be derived from Δc_p as,

$$\Delta H(t_A, \infty) = \Delta c_p \times \left(T_g - T_A \right). \tag{4}$$

$\Delta H(t_A, T_A)$ has a relation with $\Delta H(\infty, T_A)$.

$$\Delta H(t_A, T_A) = \Delta H(\infty, T_A) \times (1 - \phi). \tag{5}$$

It follows that ϕ is determined from the values of $\Delta H(t_A, T_A)$ and $\Delta H(\infty, T_A)$ for a given t_A and T_A.

3. Results

The heating DSC curve for PCB6A–C is shown in Fig. 1 for $T_A = 13$ and 28 °C. It is important to estimate the uncertainties of the DSC curves because most of the data discussed in this paper are directly derived from the DSC curves. As reported below, the power law behaviour of the convex curves in the $-\ln\phi$ vs. t_A plot could be observed, especially for a low T_A measurement. To ensure data accuracy, the series of DSC scans are repeated three times. The results showed that the heat flow curves of repeated scans were in good agreement within the temperature ranges of 0–25 °C and above 50 °C, showing that the baselines before and after the glass transition did not shift. As for the area bounded by the heat flow curves, the error found by the three repeated scans for the series of $t_A = 177$–5456 min, $T_A = 13$ °C of PCB6A–C (sample weight = 14.10 mg) was less than 180 mJ/g. The scattering of 180 mJ/g coincides with that of 0.032 at the level of $-\ln\phi$ shown in Fig. 2. Although this error level is not satisfactorily low, the accuracy of the present method is within the permissible range, and further analyses of deriving AES parameter were carried out.

Three values of $-\ln\phi$ acquired by respective ageing experiments were averaged, and the results were plotted double-logarithmically against t_A in Fig. 2 to verify which approximation, the straight line or the convex curve, was more suitable. The largest and the smallest ones of the three values of $-\ln\phi$ are shown in Fig. 2 with the error bars. Consequently, the decay forms of the upward convex curve were observed for the four samples in the ageing experiments of low T_A. The experiment of $T_A = 13$ °C was not carried out for PCB6A–B. The data of the convex curve were replotted as $\log\phi$ vs. $\log(t_A)$ to fit the power function of Eq. (2); therefore, the parameters of A and n were derived for the low T_A experiments of $T_A = 18$ and 13 °C. Plots of the straight line were found for other ageing

Table 1
Molecular weight, specific heat increment, and glass transition temperature of PCB6A samples. List of parameters based on the plots shown in Fig. 2.

Sample code	M_w	M_w/M_n	$\Delta c_p/Jg^{-1}$ °C^{-1}	T_g/°C	Parameters[a]					
					Stretched exponential decay			Power law decay		
					β	τ/min	$\lvert r \rvert$	A/min^n	n	$\lvert r \rvert$
B	2×10^5	1.8	0.32	39	0.414 ± 0.048	1070 ± 100	0.993	1.88 ± 0.15	0.134 ± 0.015	0.991
C	6.5×10^4	1.3	0.31	39	0.400 ± 0.053	1290 ± 130	0.998	1.25 ± 0.19	0.049 ± 0.004	0.997
D	3.1×10^4	1.4	0.31	39	0.418 ± 0.044	1120 ± 80	0.997	1.22 ± 0.10	0.052 ± 0.016	0.991
E	1.2×10^4	1.2	0.31	36	0.376 ± 0.040	2260 ± 330	0.996	1.27 ± 0.12	0.065 ± 0.016	0.993

[a] Determined by applying Eqs. (1) and (2) to the plots of Fig. 2, in which T_A of the plot is indicated for the respective sample.
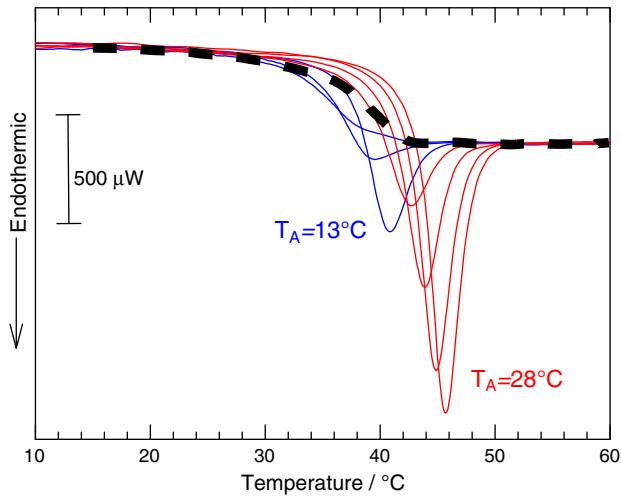
Fig. 1. Heating DSC curves of PCB6A–C with the ageing of $T_A = 13$ °C and $T_A = 28$ °C and without the ageing (thick dashed line). The ageing times were $t_A = 598$, 1257, and 5456 min ($T_A = 13$ °C) and $t_A = 117$, 597, 2637, and 5458 min ($T_A = 28$ °C) in order of decreasing intensity. Data of $t_A = 177$ ($T_A = 13$ °C) and 57 min ($T_A = 28$ °C) are excluded for simplicity.

experiments, $T_A = 28$, 23 °C for PCB6A–B and $T_A = 28$–18 °C for the other three samples. Of these results, some selected data were added to Fig. 2 to contrast the convex line with the straight line. From the slope and the intercept of the linear function, the parameters of β and τ were determined for further analyses. The values of

β, τ, A, and n were summarised in Table 1 with the uncertainties estimated using the error bars. The correlation coefficients of the linear approximations, $|r|$, that are larger than 0.990, are also added to Table 1.

As a matter of fact, it is sometimes difficult to distinguish the linear relationship from the convex curve since the curve gradually moves closer to a straight line as the parameter A of Eq. (2) increases [20]. These plots were all interpreted as straight lines in an earlier study [10]. However, it can be seen now that the plots that appeared are clearly different from the linear relation even if the uncertainties of the error bar are taken into account. The simple plot of ϕ vs. $\log(t_A)$ was also tested for the data of all the ageing experiments. As for PCB6A–B, the decay curve of $T_A = 28$ °C was basically similar to that of $T_A = 18$ °C: it was approximately linear and slightly sigmoidal over the ϕ vs. $\log(t_A)$ plot. The tendencies were the same in the plots for the three other samples. It is not easy to determine the stretched exponential regime or power law regime using the ϕ vs. $\log(t_A)$ plot.

Concerning the stretch exponent, β, it is expected to decrease with the increase in M_w, as can be observed for the dielectric relaxation processes [21], because the geometrical constraints and the slow dynamics are more pronounced to lead to the broadening of the distribution of relaxations for the polymers of the longer backbone. However, the correlation between β and M_w could not be clearly observed in this work. It is likely that the data of β obtained from the DSC experiment disagree with the data of dielectric relaxation [22]. In addition, for τ and A, no clear correlation with M_w was observed (see Table 1). As written below, both τ and A are the parameters used to characterise the relaxation rate. In practice, the main factor, i.e., the dynamics of the polymer chain, has not been revealed
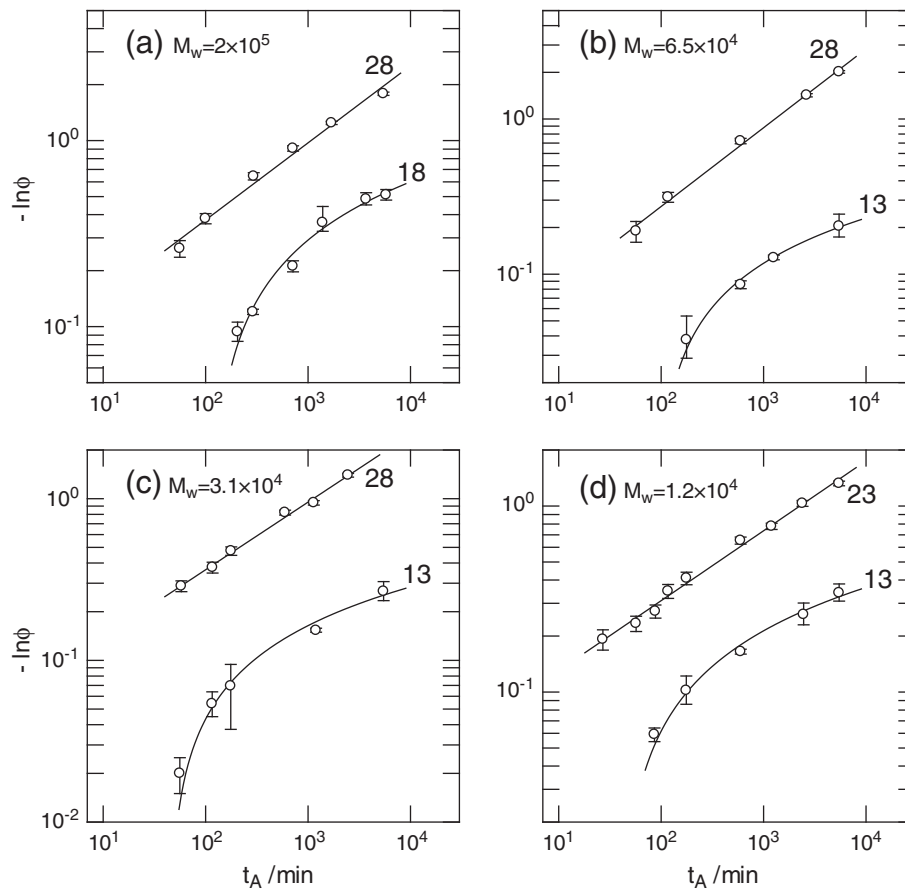
Fig. 2. Double logarithmic plots of $-\ln\phi$ vs. t_A for PCB6A samples of several fractions. M_w is displayed in the figure. Numbers denote the ageing temperature (°C). The straight lines are drawn by fitting the data with $y = a + b \times \ln x$. The upward convex curves are drawn using $\ln y = a + b \times \ln x$. The correlation coefficients in the fitting, $|r|$, for the respective lines are shown in Table 1.

for the decrease in $\Delta H(t_A, T_A)$. It is even possible that the dynamics in the short segment of the polymer is the main factor and is not involved in the geometrical constraints. It seems difficult to interpret the behaviour of τ or A with respect to M_w, with no information about the dynamics of polymer.

The fact that the power law appears in the relaxation function seems to be highly relevant to the intensity and the temperature region of the overshoot of the DSC curve. As shown in Fig. 1, the intensities of the overshoots that appeared in the experiments of $T_A = 13\ °C$ are obviously different from those of $T_A = 18\ °C$. The temperature regions in which the overshoots are located also differ; those of $T_A = 13\ °C$ are roughly located within the range of the glass transition shoulder, whereas those of $T_A = 28\ °C$ are outside the shoulder range. In addition, the calculation of $(c_{p,age} - c_{p,ref})$ produces a negative value in the range of ca. 32 to 42 °C for the DSC curve of $T_A = 28\ °C$. On the other hand, the negative value in $(c_{p,age} - c_{p,ref})$ does not appear at all for the DSC curve of $T_A = 13\ °C$. The intensity, temperature region, negative value in $(c_{p,age} - c_{p,ref})$, the origin of these observed features comes mainly from the thermodynamic state immediately after the isothermal stage. More specifically, the change of the configurational entropy and the internal enthalpy in the ageing process severely affects the way in which the overshoots appear [11]. It follows that the samples showed the enthalpy decay with a different relaxation function according to the different ageing temperatures, resulting in different types of overshoots.

4. Discussion

The decrease in enthalpy caused by thermal ageing is the approach to the equilibrium state at T_A and is controlled by molecular processes. According to the AES model, the molecular processes are activated with the energies, E having the distribution over a continuous spectrum. $\Delta H(t_A, T_A)$ can be obtained by the integral of Eq. (6),

$$\Delta H(t_A, T_A) = \int_0^{kT_A \ln(\nu_0 t_A)} P(E)dE, \qquad (6)$$

where $P(E)$ is the enthalpy change related to relaxation processes having activation energies in the range of $E + dE$ [15]. The process contributes to the decrease in enthalpy after the time of t_A. Usually, without loss of generality, the processes may be regarded as being all of one type with a single average value of $c(E)$, and, therefore, $P(E)$ expresses the number density of processes in the structural relaxation. ν_0 is the frequency

factor for single atom processes and is derived from the frequency of the Debye temperature, $\theta_D = (h \times \nu_D)/k$; h and ν_D are Planck's constant and the Debye frequency, respectively. Eq. (7) can be derived from Eqs. (5) and (6); it follows that the activation energy spectrum of the relationship between $P(E)$ and E can be calculated.

$$P(E) = -\frac{\Delta H(\infty, T_A)}{kT_A} \cdot \frac{d\phi}{d \ln t_A}\bigg|_{t_A = \frac{1}{\nu_0} \exp\frac{E}{kT_A}}. \qquad (7)$$

Fig. 3(a) shows the AES based on the linear relations of the double logarithmic plots of $-\ln\phi$ and t_A, shown in Fig. 2. The AES obtained with the relaxation function of the power law is shown in Fig. 3(b), taking the parameters A and n from the upward convex curve in Fig. 2. As a result, the spectrum derived from the decay function of the stretched exponential form was entirely different from that of the power law decay.

In the AES derived from the stretched exponential decay, the peak position and peak height are nearly identical for the four samples, as shown in Fig. 3(a). In general, the peak position is exclusively influenced by τ, more precisely, by $\log(\tau)$. Although the τ value of the decay function of PCB6A–E is roughly twice that of the other sample, it has less influence on the peak position due to the log of τ. The factors to determine the peak height are β and $\Delta H(\infty, T_A)$. As β approaches 1, the peak width decreases, and the peak height increases, or vice versa as β approaches 0. Although β of the decay function of PCB6A–E is the smallest value in the results shown in Table 1, a larger $\Delta H(\infty, T_A)$ makes its peak higher than other peaks. As a consequence, in this work, the energy distributions are almost identical among the samples for the molecular processes of the relaxations expressed by the stretched exponential decay in Fig. 2. The result that the energy range is from 60 to 110 kJ/mol is roughly comparable with the data of the enthalpy relaxation reported for the liquid crystalline polymer of the main-chain type [23].

The AES derived from the power law decay shows an attenuation curve with a reduction such as the inverse proportion, showing that the process activated by low energy accounts for most of the total processes and the population decreases rapidly towards the higher energy side. The intercept in the ordinate and the energy upper limit in which the AES curve meets with the abscissa can be taken as the characteristics of the spectrum. Since no other studies have been published reporting the AES calculated from the power law decay, a short discussion on the relaxation function is presented here. There are few examples in which the power law dependence is observed in
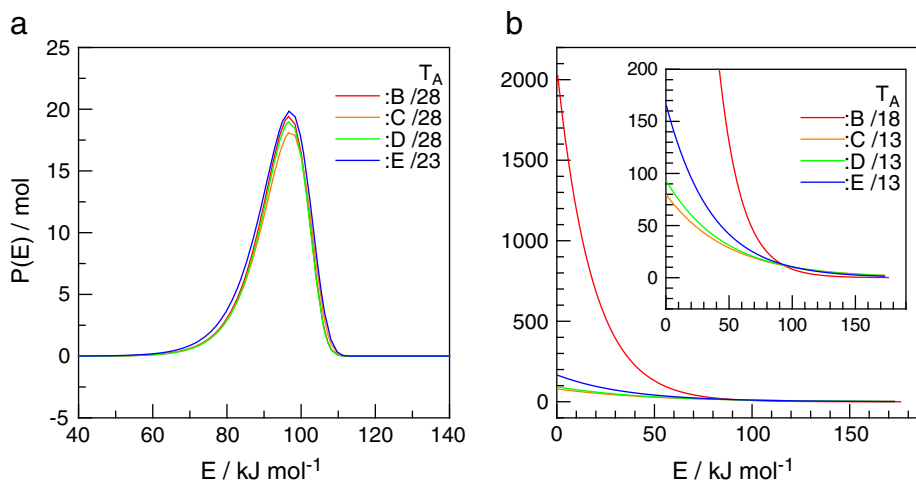

Fig. 3. Activation energy spectra for the enthalpy relaxations based on the plot of Fig. 2. (a) The stretched exponential function was applied to derive AES for four PCB6A samples. Numbers denote the ageing temperature (°C). (b) The power law dependence was applied to derive AES. Numbers denote the ageing temperature (°C).

the relaxation phenomenon. To the author's knowledge, two examples can be raised, i.e., the particle diffusion in fractional Brownian motion and the stress relaxation modulus in the liquid–solid transition [24,25]. Therefore, Eq. (2) is accounted for by following the example of the relaxation modulus. We may simply understand that A is the decrease rate, for A is the relaxation amount when $t_A = 1$ s. The expression of A as $A = \phi \times (t_A)^n$ may be of help to understand the physical meaning of A. A has an unusual unit of $(\min)^n$. n characterises the power law distribution of the mode of the relaxation process. The relaxation processes of different modes are not independent of each other but, rather, coupled [26,27]. The coupling influences the n value. Moreover, it is noteworthy that the value of ϕ of Eq. (2) does not start from 1 in spite of the fact that the relaxation function generally takes the value of 1 as $t_A = 0$.

The influence of A and n on the AES curve appears in the intercept and the energy upper limit. The upper limit shifts to the higher side as A increases. As n increases, the intercept becomes higher, and the slope, steep. In particular, the intercept depends largely on the n value. The result that the AES curve of PCB6A–B stands out to show a higher value comes from the larger values of both A and n recorded in comparison with other ageing experiments of PCB6A samples. No legitimate idea could be given within the limited data in this work, showing the reason for the larger values in A and n being recorded. However, one possibility is that T_A used for the ageing of PCB6A–B was higher than that used in other ageing experiments.

The data obtained in this work accurately describe the enthalpy relaxations of both the stretched exponential decay and the power law decay. However, in general, it is inconceivable that two or more relaxation functions appear in the particular material. At least, the coexistence of two kinds of relaxation functions has not been reported elsewhere. In this regards, Hodge has described the generalisation from a sufficiently large collection of experimental data, that the behaviour of such properties as $\Delta H(t_A, T_A)$, the temperature of heat capacity maximum, etc. varies if the aged glass is much far from the equilibrium or it is close to the equilibrium[28]. It is possible that two kinds of functional forms can be observed if we consider the suggestion that close relations are seen between the decay function and these properties. For example, ageing experiments with short intervals in T_A to observe the continuous variation between the two functions will be of help to demonstrate the coexistence of two kinds of functions. Furthermore, it is necessary to propose some molecular mechanism of the power law relaxation in addition to observing the phenomenon. Needless to say, the power law implies self-similarity in the time domain, yet the dynamics of the relaxation components are not clarified. The relation between the relaxation modes of motion of a polymer chain and the respective activation energy might be of help to explain the molecular mechanism.

References

[1] J.D. Ferry, Viscoelastic Properties of Polymers, Wiley, New York, 1980.
[2] R. Rodriguez, M. Estevez, S. Vargas, J. Non-Cryst. Solids 357 (2011) 1383–1389.
[3] K.L. Ngai, J. Non-Cryst. Solids 353 (2007) 709–718.
[4] K.L. Ngai, Relaxation and Diffusion in Complex Systems, Springer, 2011. , (Chap.2).
[5] I. Avramov, I. Gutzow, J. Non-Cryst. Solids 298 (2002) 67–75.
[6] T.A. Vilgis, H.H. Winter, Colloid Polym. Sci. 266 (1988) 494–500.
[7] S.P. Das, J. Chem. Phys. 105 (1996) 8822–8825.
[8] S. Srivastava, S.P. Das, Phys. Rev. E 63 (2001) 011505.
[9] D. Chakrabarti, P.P. Jose, S. Chakraborty, B. Bagchi, Phys. Rev. Lett. 95 (2005) 197801.
[10] Y. Tanaka, Polym. J. 39 (2007) 1030–1039.
[11] Y. Tanaka, T. Yamamoto, J. Non-Cryst. Solids 358 (2012) 1687–1698.
[12] D. Lacey, G. Nestor, M.J. Richardson, Thermochim. Acta 238 (1994) 99–111.
[13] C. Alvarez, N.T. Correia, J.J. Moura Ramos, A.C. Fernandes, Polymer 41 (2000) 2907–2914.
[14] L. Andreozzi, M. Faetti, M. Giordano, D. Palazzuoli, Macromolecules 35 (2002) 9049–9056.
[15] M.R.J. Gibbs, J.E. Evetts, J.A. Leake, J. Mater. Sci. 18 (1983) 278–288.
[16] A.S. Marshall, S.E.B. Petrie, J. Appl. Phys. 46 (1975) 4223–4230.
[17] S.E.B. Petrie, J. Polymer Sci. A2 (10) (1972) 1255–1272.
[18] S. Montserrat, P. Colomer, J. Belana, J. Mater. Chem. 2 (1992) 217–223.
[19] J.L. Gómez Ribelles, A. Ribes Greus, R. Díaz Calleja, Polymer 31 (1990) 223–230.
[20] L. Kirkup, Experimental Methods: An Introduction to the Analysis and Presentation of Data, J. Wiley&Son, Brisbane, 1994. , (Chap.3).
[21] C. Leon, K.L. Ngai, C.M. Roland, J. Chem. Phys. 110 (1999) 11585–11591.
[22] J.M. Meseguer Dueñas, A. Vidaurre Garayo, F. Romero Colomer, J. Más Estellés, J.L. Gómez Ribelles, M. Monleón Pradas, J. Polym. Sci., Part B: Polym. Phys. 35 (1997) 2201–2217.
[23] V. Lorenzo, J.M. Pereña, E. Pérez, R. Benavente, A. Bello, J. Mater. Sci. 32 (1997) 3601–3605.
[24] T.G.M. van de Ven, J. Colloid Interface Sci. 62 (1977) 352–355.
[25] H.H. Winter, M. Mours, Adv. Polym. Sci. 134 (1997) 165–234.
[26] H.H. Winter, F. Chambon, J. Rheol. 30 (1986) 367–382.
[27] F. Chambon, H.H. Winter, J. Rheol. 31 (1987) 683–697.
[28] I.M. Hodge, Macromolecules 16 (1983) 898–902.